ELSEVIER

Clinical Biomechanics 17 (2002) 185–196

CLINICAL BIOMECHANICS

www.elsevier.com/locate/clinbiomech

Force-deformation response of the lumbar spine: a sagittal plane model of posteroanterior manipulation and mobilization

Tony S. Keller [a,*], Christopher J. Colloca [b], Jean-Guy Béliveau [c]

[a] *Department of Mechanical Engineering, Department of Orthopaedics and Rehabilitation, University of Vermont, 119C Votey Building, Burlington 05405-0156, Vermont, USA*

[b] *Postgraduate and Continuing Education Department Faculty, New York Chiropractic College, Seneca Falls, New York, USA, State of the Art Chiropractic Center, P.C., Phoenix, AZ, USA*

[c] *Department of Civil and Environmental Engineering, University of Vermont, Burlington, Vermont, USA*

Received 9 January 2001; accepted 10 January 2001

Abstract

Objective. To develop a mathematical model capable of describing the static and dynamic motion response of the lumbar spine to posteroanterior forces.

Design. Static, impulsive and oscillatory forces with varying thrust angles and offsets were applied to the model, and the resulting motion responses were compared to experimental data published for spinal mobilization and manipulation of prone-lying subjects.

Background. Methods are sought to improve understanding of the dynamic force-induced displacement response of the lumbar spine during spinal mobilization and manipulation treatment.

Methods. The thorax, pelvis and five lumbar vertebrae were represented as seven rigid structures and eight flexible joint structures. Flexible joint structures were modeled using spring and damper elements with three displacement degrees-of-freedom (posterior–anterior and axial displacement, and flexion–extension rotation). The resulting 21 degrees-of-freedom lumped parameter model was solved in modal space.

Results. The fundamental natural frequency of vibration was 5.24 Hz. Simulations performed using 100 N static and dynamic posteroanterior forces applied to the L3 vertebrae indicated that peak L3 segmental displacements were up to 2.40 mm (impulsive) and 8.23 mm (oscillatory at 2 Hz). Appreciable axial displacements (0.41 mm) and flexion–extension rotations (1.49°) were also observed for oscillatory forces at L3. The posteroanterior motion response of the lumbar vertebrae was relatively insensitive to both the thrust force angle and thrust force offset, but axial displacements and flexion–extension rotations showed a large change (2-fold or greater) for thrust angles greater than −5° (caudal) in comparison to vertical thrusts. Intersegmental motion responses for static, impulsive and oscillatory loads were more comparable than their segmental counterparts.

Conclusions. The model predicts lumbar segmental and inter-segmental motion responses to manipulative forces that are otherwise difficult to obtain experimentally.

Relevance

This study assists clinicians to understand the biomechanics of posteroanterior forces applied to the lumbar spine of prone-lying subjects. Of particular clinical relevance is the finding that greater spinal mobility is possible by targeting specific load-time histories. © 2002 Elsevier Science Ltd. All rights reserved.

Keywords: Biomechanics; Dynamic simulation; Lumbar spine; Manipulation; Model; Natural frequency; Rigid body; Spine; Vibration

1. Introduction

Numerous spinal manipulative therapy techniques exist that involve the application of posteroanterior (PA) forces of different magnitudes, loading directions, and loading rates to prone-lying patients. In addition to treatment application, clinicians commonly apply oscillatory PA forces to the spine to assess its mobility, stiffness, or to note the effect of applied force on the patient's symptoms. In spite of the fact that external forces are routinely applied to the spine during the clinical course of assessments and therapy, very little is known about the mechanics of such procedures [1]. Noteworthy is the fact that forces applied to the spine

* Corresponding author.
E-mail address: keller@emba.uvm.edu (T.S. Keller).

0268-0033/02/$ - see front matter © 2002 Elsevier Science Ltd. All rights reserved.
PII: S0268-0033(02)00003-7

Nomenclature

M	system mass matrix
C	system damping matrix
K	system stiffness matrix
u	displacement vector
F	force vector
l	segment link dimensions (m)
m	segment mass (kg)
X_0	initial x-axis disp. (m)
H	frequency response function
$\bar{F}$	static force
t	time (s)
ϕ	mode shape matrix
I	identity matrix
Ω	natural frequency vector
ξ	modal damping ratio
a	spring axis constant (m)
ω	natural frequency (rad/s)
Y_0	initial y-axis disp. (m)
M_z	torsion moment (Nm)
$\hat{F}$	impulsive force
tr	transpose
φ	thrust angle (rad)
e	thrust eccentricity (m)
k_x	axial stiffness (N/m)
k_y	transverse stiffness (N/m)
κ_z	torsion stiffness (N/m)
v_0	initial velocity (m/s)
F_0	initial force (N)
θ	rotation angle (rad)
$\tilde{F}$	oscillatory force

during mobilization and manipulation are generally dynamic or time varying in nature. Indeed, the time duration of chiropractic force–time profiles may range from approximately half a second for low frequency sinusoidal oscillations [2] and single haversine manual thrusts [3,4] to less than five milliseconds during some mechanical force techniques [5–7]. The dynamic mechanical aspects of these procedures are poorly understood. Thus, reliable methods to obtain an adequate understanding of the force-induced motion response of the spine have long been considered important.

Without resorting to invasive measurement techniques, the precise assessment of clinically relevant variables such as vertebral and intervertebral movements are very difficult to obtain [8]. Consequently, the development of mathematical or numerical models to characterize the biomechanical behavior of the spine is an important step toward understanding the theoretical basis for mobilization and manipulation. Lee et al. [9] were perhaps the first investigators to develop a mathematical model to specifically study the lumbar spine's response to posterior-anteriorly directed forces. Subsequently, Lee et al. [8] developed a three-dimensional finite element model of the spine, ribcage, and pelvis, which was used to predict static segmental displacement responses of the lumbar vertebrae to PA forces. They validated their model by comparing predictions to low frequency (<1 Hz) PA oscillatory force–displacement data observed in human subjects and found generally good agreement with the mean responses. One advantage of such biomechanical models is the ability of such models to study the mechanical response of the spine under a wide variety of different loading environments. Solinger [10] recently used an analytical model to describe the dynamics of small impulses applied to a single vertebral motion segment. In that study, experimental data was used to identify system parameters (such as stiffness and damping), but the author did not consider coupling between adjacent vertebrae. As a first step toward developing a more complete understanding of the static, dynamic and impact mechanical response of the lumbar spine to PA forces, Keller and Colloca [11] developed a five degree-of-freedom (DOF) analytical model of the vertebral and intervertebral motion response of the lumbar spine. This model was limited to predicting the vertebral and intervertebral motion responses along a single axis (PA) and did not consider the influence of the thorax and pelvis.

The objective of this paper was to develop a more comprehensive mathematical model capable of describing the coupled flexion–extension (FE) rotation, axial (cranial-caudal) and transverse or posteroanterior (PA) vertebral and intervertebral motion response of the lumbar spine, pelvis and thorax of prone-lying subjects. Results are presented for static, oscillatory and impulsive forces applied posterior-anteriorly along different sagittal plane force vectors. Model predictions are discussed in context with in vivo measurements of vertebral motion subjected to various spinal manipulative and mobilization forces.

2. Methods

All structures possessing mass, elasticity and finite damping are capable of vibration. From an engineering point-of-view the basic vibration model consists of a mass, a massless spring (elastic element), and a damper (viscous element). Many viscoelastic structures, including the vertebral column, contain more than one mass, in which case more than one set of coordinates and properties need to be specified to describe its static and dynamic mechanical properties. Of particular interest for such systems are the natural frequency of vibration

and the motion response of the system to external or forced excitation. In the analysis that follows, the five lumbar vertebral segments, thorax and pelvis are modeled as rigid structures connected by six, flexible joint structures (FJS). The vertebral joint structures consist of the intervertebral discs and other soft connective tissues (ligaments, muscles, tendons, and cartilage) that comprise the anterior and posterior columns of the functional spinal unit. The mass of the vertebral segments and FJS are lumped together, elasticity and viscous properties of the flexible couplings are specified, and the motion of the rigid structures is expressed in terms of the motion of the thorax, pelvis and each lumbar vertebrae.

A mass, massless-spring and damper model of the human lumbar spine, pelvis and thorax of a prone-lying subject is shown in Fig. 1. This model has three sagittal plane displacement DOF for each lumbar segment, thorax and pelvis (sacrum). Modeling of this multi-DOF structure necessitates one governing differential equation of motion for each DOF, together with specifications for the mass matrix $[M]$, damping matrix $[C]$, stiffness matrix $[K]$, and input excitation force vector $\{F\}$. The matrix representation of the differential equations of vibration of the spine structure is:

$$[M]\{\mathrm{d}^2u/\mathrm{d}t^2\} + [C]\{\mathrm{d}u/\mathrm{d}t\} + [K]\{u\} = \{F\}, \qquad (1)$$

where $\{u\}$ is the resulting displacement output vector (column matrix).

In the model presented here, the dynamic motion response of the five lumbar vertebral segments, the pelvis (sacrum) and the thorax are determined for each of the following sagittal plane axes: axial (x), PA or transverse (y) and FE rotation (z). Since each of the seven segments has three displacement DOF (x, y, z), the model has a total 21 DOF. We assumed that the system has zero mass coupling, in which case the mass matrix

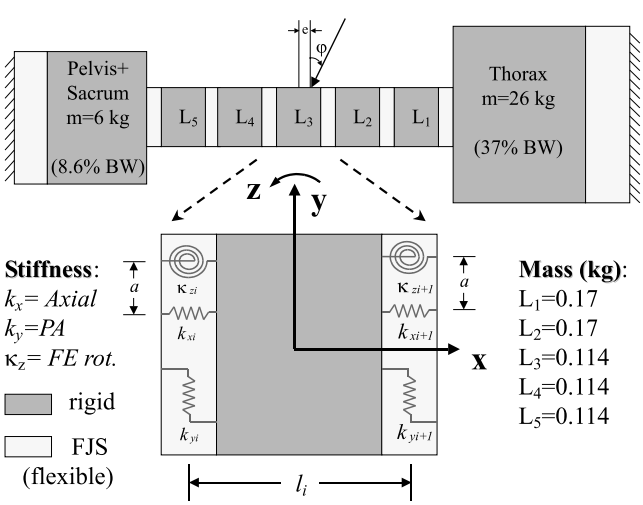

Fig. 1. Lumped equivalent model of the lumbar spine, pelvis and thorax. Damping elements are not shown for purposes of clarity.

$[M]$ is diagonal. We also assumed that the vertebral segments, pelvis (sacrum) and thorax were rigid structures connected by flexible, massless linkages. Because the elasticity or stiffness characteristics of the flexible linkages are specified according to the literature values for the transverse (PA), axial and FE rotation stiffness characteristics of intact lumbar and lumbar-sacrum motion segments [12], the linkages (FJS) represent the collective properties of the anterior joint structures (intervertebral discs, IVD), posterior joint structures (facets), and other connective tissues (ligaments). Axial and transverse stiffness characteristics of the thorax were based on the axial stiffness of the T12 thoracic vertebra and transverse stiffness of the rib cage, respectively [12]. The FE rotation stiffness of the thorax was assumed to be equal to 2.5 times the FE rotation stiffness of the thoracic spine, since the rib cage increases the rotational stiffness of the thoracic spine by this amount [12]. The patient is assumed to lie in a relaxed, prone position supported by the thorax and rib cage and anterior superior iliac spine. The equations of motion (Eq. (1)) assume that the abdominal cavity tissues and skin overlying the pelvis and thorax are more compliant than the spine structures and therefore do not contribute significantly to the overall stiffness of the spine, thorax and pelvis.

The stiffness matrix $[K]$ was formulated in terms of the stiffness influence coefficients and the resulting stiffness matrix is a 21×21 matrix comprised of nine tri-diagonal sub-matrices (see Appendix A). The model can accommodate eccentrically applied forces (producing moments) directed to any segment at an arbitrary thrust angle (φ) and with a thrust offset or eccentricity e (see Fig. 1).

Table 1 summarizes the axial (k_x), transverse (k_y) and torsion (κ_z) stiffness coefficients used to model the eight FJS (six IVD's, pelvis + sacrum and thorax). The axial and torsion spring axes were coupled using a spring axis constant (a). Masses and segment link dimensions for each of the seven segments were based on a 70 kg body weight, 170 cm body height reference man [13]. Segment masses are given in Fig. 1 and segment link dimensions (l) were defined as: 0.1240, 0.0355, 0.0375, 0.0390, 0.0400, 0.0390, and 0.0410 for thorax, L_1, L_2, L_3, L_4, L_5 and pelvis + sacrum, respectively. The axial and torsion spring axis coupling constant was assumed to be 20 mm for all FJS's [14].

The equations of motion are solved in modal space using the eigensolution (i.e. the modal properties) of the homogeneous equation of motion (free vibration without damping). The eigenvectors (mode shapes) are then assembled into a mode shape matrix $[\phi]$ such that $[\phi]^{\mathrm{tr}}[M][\phi] = [I]$ and $[\phi]^{\mathrm{tr}}[K][\phi] = [\Omega^2]$, where tr denotes the transpose, $[I]$ is the diagonal identity matrix, and Ω is a vector of the natural frequencies of vibration. Given the modal damping ratios ζ_i for each mode shape i, the

Table 1
Summary of model flexible joint structure stiffness coefficients corresponding to the axial (x), transverse (y) and flexion–extension rotation (z) axes of each segment

Stiffness coefficient	Thorax	T12–L1	L1–L2	L2–L3	L3–L4	L4–L5	L5–L1	Pelvis and sacrum
k_x (kN/m)	1250	640	620	600	525	450	510	300
k_y (kN/m)	30	50	40	35	30	30	45	200
κ_z (Nm/rad)	400	160	140	120	100	80	75	700

21×21 damping coefficient matrix is formulated as $[C] = [M][\phi]2[\zeta][\Omega][\phi]^{\mathrm{tr}}[M]$. Examination of intersegmental displacement–time profiles obtained during the application of mechanical force, manually assisted thrusts to the lumbar spine [6] suggest that damping ratios can be up to 30% of critical. In the analysis that follows, the modal damping ratios for each segment were assumed to be identical: $\zeta_{1,\ldots,7} = 0.25$ (25% of critical).

Although a detailed parametric examination of the model dependency on structural properties is beyond the scope of the present study, we note that variation of K, M, ζ, l and a will produce significant changes in the natural frequency of vibration and motion response of the model. Variations in structural and geometric properties are expected as a natural consequence of height and weight variations in female and male subjects, as well as factors associated with aging, activity level and disease. The parameters K, M, ζ, l and a chosen for this study are intended to be representative of a 70 kg body mass, 170 cm tall male subject.

2.1. Applied forces

Manual therapeutic forces can be broadly classified into several categories, however, the most commonly used procedures among clinicians include spinal mobilization, and high velocity, low amplitude manipulation. Manipulation can be further categorized as specific contact thrust procedures (delivered by hand), and mechanical force, manually assisted procedures (delivered by means of a mechanical device), although many more forms of manipulation application or chiropractic techniques exist [15]. Spinal manipulative techniques direct forces PA, in combination with other vectors in a variety of patient positions (prone, supine, and side posture). In the analysis that follows, only sagittal plane PA forces and concomitant motions in the lumbar spine are examined.

Mobilization is commonly used during both the assessment and treatment of spinal disorders and involves applying low frequency (0.05–2 Hz) oscillatory PA forces to a selected vertebra or several vertebrae with the patient lying prone [16]. Both manual and instrument-based mobilization assessments and treatments exist [17,18]. Peak mobilization forces applied to the lumbar spine typically range from 100–200 N [2]. During mobilization, the spine is forced to vibrate at the same frequency as that of the excitation, and *steady-state* oscillations are produced.

Spinal manipulation involves a specifically vectored high velocity, low amplitude thrust that is usually directed in a PA direction [4]. Hence, spinal manipulation differs from mobilization in that the spine is influenced by a suddenly applied non-periodic excitation. Such excitations are called *transient* since steady-state oscillations are generally not produced. Manual manipulation applied to the thoraco-lumbar spine are generally associated with higher peak PA forces (typically 250–550 N), but are comparable to mobilization therapy in terms of time to peak force (typically 100–200 ms) [3,19]. Mechanical force, manually assisted procedures utilize a hand-held mechanical instrument to produce a very short duration (typically <5 ms) force–time profile with peak force amplitudes ranging from 100–200 N [5]. Forces that are relatively large in magnitude, but act for a very short time (much less than the natural period of oscillation), are called *impulsive*. Impulsive forces $\hat{F}$ acting on a mass m will result in a sudden change in velocity equal to $\hat{F}/m$, but are typically associated with smaller displacements in comparison to longer duration transient forces.

Using Matlab (The Mathworks, Natick, MA, USA), the vertebral (segmental) and intervertebral (intersegmental) motion responses of the lumbar spine, pelvis and sacrum were studied in response to forces consistent with the aforementioned common forms of mobilization therapy and spinal manipulation. The effects of preload, which is commonly employed in chiropractic treatments, will not be considered in the analysis that follows. Six sagittal plane thrust angles and 6 thrust offsets were examined in this study: 5° to −20° (toward pelvis) and 0–2.5 cm (toward pelvis), respectively. In each case a 100 N peak excitation force was applied to the spinous process of the L3 vertebral segment. In addition to model validation using low cycle human in vivo mobilization studies [2,16,18,20–24], the model displacement results are compared to previously published in vivo intersegmental displacement responses obtained for human subjects in response to impulsive manipulative thrusts in an outpatient setting [6] and in a surgical setting [25]. The dynamic frequency response characteristics of the model are also validated with respect to previous in vivo transient vibration studies conducted using human volunteers [26].

3. Results

The undamped frequencies predicted by the model for the first 14 of 21 modes of vibration were 5.24, 17.7, 26.8, 35.9, 40.6, 44.8, 77.0, 116, 124, 140, 158, 177, 196, 260 Hz. Thus, the fundamental natural frequency or first resonant frequency for the thorax-lumbar spine-pelvis model was 5.24 Hz. Examination of the model-predicted mode shapes indicated that the natural frequencies of vibration for the posterior–anterior axis (y), FE rotation axis (z), and axial axis (x) of the lumbar segments were 40.6, 77 and 124 Hz, respectively. The damped ($\zeta = 0.25$) natural frequencies of vibration for these three coordinate axes were 39.3, 74.5 and 120 Hz.

3.1. Static response

The model predicted static displacement response $\bar{u}$ to PA static forces $\bar{F}$ is the solution to the equation $[K]\{\bar{u}\} = \{\bar{F}\}$ computed by Gaussian elimination. For a static force $\bar{F} = 100$ N applied only to the L3 vertebral segment ($\varphi = 0,\ e = 0$), the PA static deformation was greatest at L3, whereas the peak axial deformation and FE rotation occurred at L5 (Fig. 2). Peak L3 segmental and L3–L4 intersegmental static deformation magnitudes for each of the coordinate axes are summarized in Table 2.

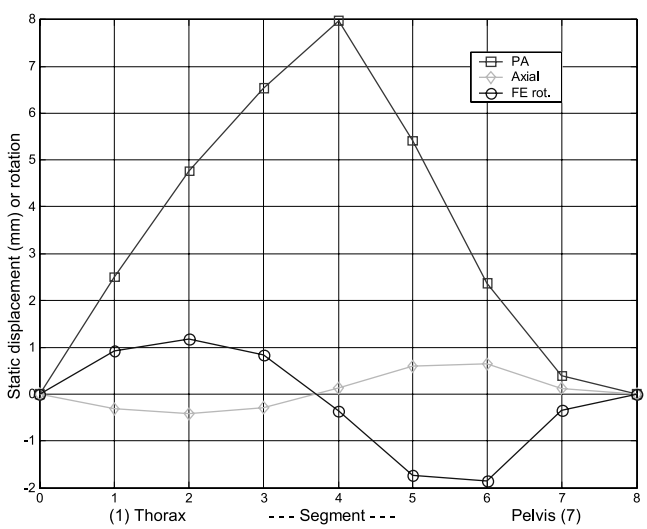

Fig. 2. Posterior–anterior displacement, axial displacement and flexion–extension rotation (FE rot.) motion responses of the L3 lumbar vertebra (segment 4) to a 100 N posterior–anterior *static* force $\bar{F}$ at L3 ($\theta = 0°$, $e = 0$ mm, $\zeta = 0.25$).

3.2. Steady-state response

The steady-state response to a PA sinusoidal input oscillation, $\tilde{F} = F_0 e^{i\omega t}$ is given by the frequency response function: $H(\omega) = [K - \omega^2 M + i\omega C]^{-1}$. $H(\omega)$ is a complex function defined as the ratio of the output displacement response to the input force under steady-state conditions. In comparison to static loading (0 Hz), the thorax exhibited the greatest increase or gain (2.1-fold at 4.9 Hz) in PA displacement response, whereas the pelvis showed the greatest gain (2.0-fold) in PA displacement at 25 Hz. Each of the lumbar segments showed an increased PA displacement response near 5 Hz, except the L5 segment, which had a maximum near 25 Hz. All of the segments showed a markedly decreased PA frequency response above 50 Hz, indicating attenuation of the PA sinusoidal oscillation above this frequency. Fig. 3 shows the predicted steady-state L3 segmental displacement response (normalized with respect to the static or DC response) for the L3 segment. Relative to the DC (0 Hz) displacement response, the maximum increase in the PA displacement, FE rotation and axial displacement occurred at 4.2, 64 and 113 Hz, respectively.

The oscillatory displacement output under steady-state conditions is given by $H(\omega)F_0 e^{i\omega t}$, where $F_0 = 100$ N amplitude applied to L3. At the damped ($\zeta = 0.25$) natural frequency (39.3 Hz) corresponding to the PA axis, the peak L3 segmental PA displacement, axial displacement and FE rotation were 7.99 mm, 0.22 mm and 0.14°, respectively. The corresponding peak–peak L3–L4 intersegmental PA displacement, axial displacement and FE rotation were 1.73 mm, 0.27 mm, and 1.49°, respectively. For sinusoidal excitation at 2 Hz the model predicts a peak–peak L3 segmental PA displacement, axial displacement and flexion extension rotation

Table 2
Baseline response of the 21 DOF model ($\varphi = 0°$, $e = 0$ m, $\zeta = 0.25$)

Loading condition	Axial displacement (mm)		PA displacement (mm)		FE rotation (degrees)	
	L3	L3–L4	L3	L3–L4	L3	L3–L4
Static force	0.131	0.472	7.97	2.55	0.374	1.35
Sinusoidal @ 2.0 Hz	0.160	0.473	8.23	2.65	0.459	1.35
Sinusoidal @ 5.2 Hz	0.412	0.224	7.67	2.45	1.20	0.632
Sinusoidal @ 39 Hz	0.223	0.276	7.99	1.73	0.141	1.49
Impulsive force	0.074	0.229	2.40	1.74	0.126	0.636

Peak-to-peak segmental (L3) and inter-segmental (L3–L4) displacement (mm or degrees) for each axis are summarized for static ($\bar{F}$), impulsive ($\hat{F}$) and sinusoidal ($\tilde{F}$) oscillatory loading conditions.

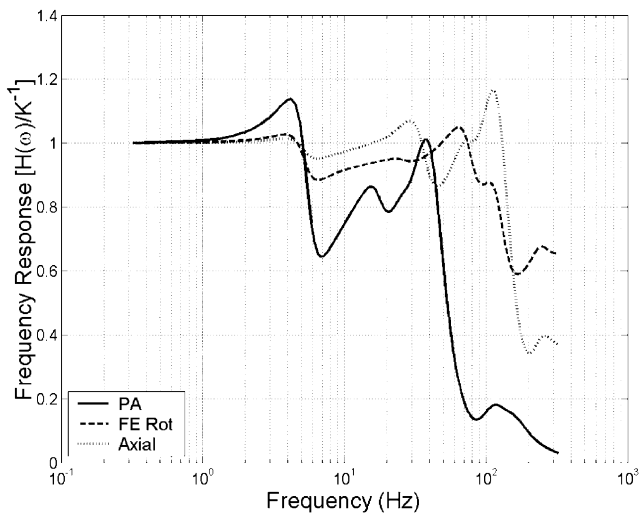

Fig. 3. L3 posterior–anterior, axial and flexion–extension rotation (FE rot.) steady-state, frequency response to a sinusoidal dynamic force $\hat{F}$ at L3 ($\zeta = 0.25$). The frequency response $H(\omega)/K^{-1}$ illustrates the increase/decrease in displacement relative to the static or 0 Hz displacement response. A frequency sweep from 0.325 to 325 Hz (increments of 0.325 Hz) is graphed using a logarithmic abscissa.

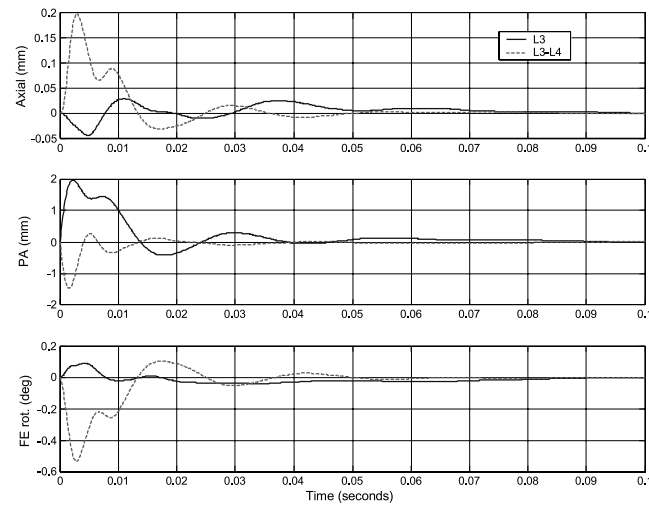

Fig. 4. Segmental (L3, solid lines) and inter-segmental (L3–L4, dashed lines) displacement responses to a 1.8414 m s^{-1} initial velocity impulsive force $\hat{F}$ at L3 ($\varphi = 0°$, $e = 0$ m, $\zeta = 0.25$).

of 8.23 mm, 0.16 mm and 0.46°, respectively. The corresponding peak–peak L3–L4 intersegmental PA displacement, axial displacement and flexion extension rotation were 2.64 mm, 0.47 mm and 1.35°, respectively.

3.3. Impulsive force response

The impulsive force response to an initial displacement $[X_0]$ and velocity $[v_0]$ was obtained by assuming a solution $X = Ue^{\lambda t}$ for the governing equation of motion (Eq. (1)). Mechanical force, manually assisted adjustments produce a damped sinusoidal type of oscillation with a total duration of approximately 0.005 s. Since mechanical force, manually assisted force–time periods are less than the natural period of oscillation, we used the impulse-momentum principle to estimate v_0 corresponding to a damped 100 N peak mechanical force, manually-assisted adjustment. Experimental force–time histories [5,7] were used to derive the following mathematical expression of the impulsive force: $\hat{F} = 466e^{-1000t}\sin(200\pi t)$. The initial velocity $v_0 = \frac{1}{m}\int F\,dt$ obtained was 1.8414 m/s. Fig. 4 illustrates the predicted axial displacement, PA displacement and FE rotation profiles produced during the application of a mechanical force, manually assisted adjustment ($X_0 = Y_0 = \theta_0 = 0$, $\zeta = 0.25$, $\varphi = 0$, $e = 0$). Note that the effect of damping is primarily the diminishing of the vibration amplitude with time, and in this system of vertebrae the impulsive force-induced oscillation were close to zero after a time period of about 100–200 ms. Model predicted L3 segmental and L3–L4 intersegmental PA peak–peak displacements were 2.40 mm and 1.74 mm, respectively.

Peak L3 segmental and peak–peak intersegmental static, sinusoidal and impulsive force motion response results for each coordinate axes are summarized in Table 2 ($\zeta = 0.25$, $\varphi = 0$, $e = 0$).

3.4. Influence of thrust angle and thrust offset

Fig. 5 summarizes the influence of thrust angle and thrust offset on the static, sinusoidal, and impulsive motion responses of the L3 segment. Both thrust angle and thrust offset produced marked changes in the axial and FE rotation segmental motion responses. Noteworthy was the finding that impulsive forces tended to produce greater axial and FE motion responses in comparison to static and sinusoidal excitation, but produced substantially lower PA motion responses. A thrust angle of +5° (cephalad) resulted in the greatest L3 static and L3 sinusoidal axial, PA and FE motion responses. Impulsive forces delivered with a thrust angle of −20° (toward pelvis) and thrust offset of 2.5 cm (toward pelvis) resulted in the greatest axial displacement and FE rotation motion response. The effects of thrust angle and thrust offset on the PA static, impulsive and sinusoidal displacement responses were minimal. Fig. 6 graphically illustrates the combined axial displacement, PA displacement and FE rotation behavior of the lumbar spine subjected to an impulsive force at L3.

4. Discussion

Application of the model to study forces applied to the L3 lumbar segment indicated that segmental displacements and rotations were appreciably greater for manual and mobilization forces in comparison to

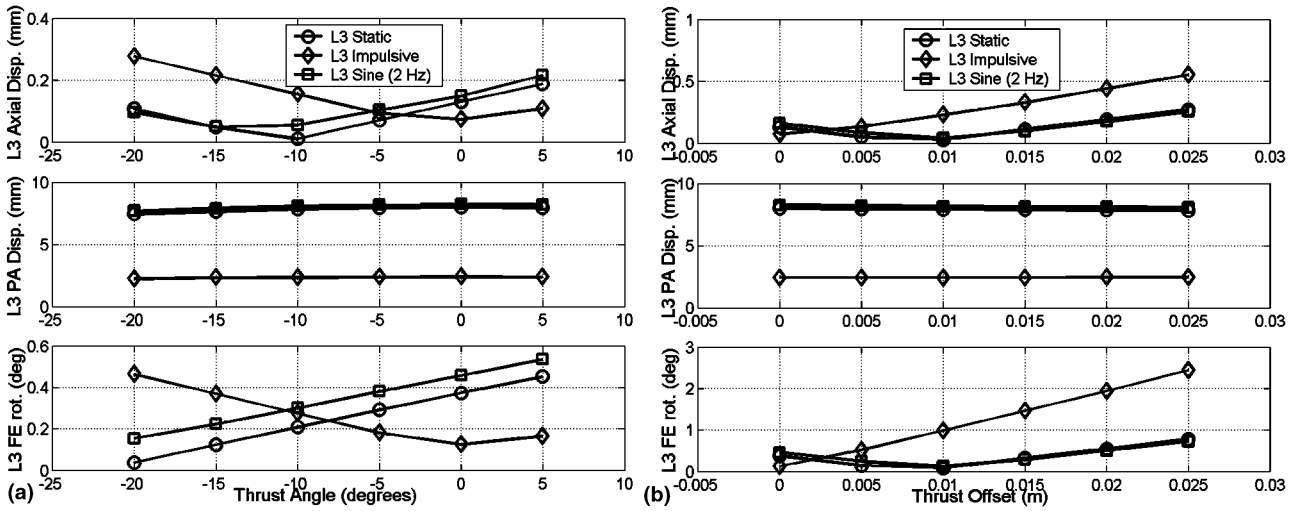

Fig. 5. (a) Influence of thrust angle (φ) on the static, impulsive and sinusoidal motion response of the L3 vertebral segment subjected to a 100 N posterior–anterior force ($e = 0$ m, $\zeta = 0.25$). (b) Influence of thrust offset (e) on the static, impulsive and sinusoidal motion responses of the L3 vertebral segment subjected to a 100 N posterior–anterior force ($\varphi = 0°$, $\zeta = 0.25$).

mechanical force and manually assisted thrusts, but differences in inter-segmental displacements were much less remarkable for these three types of spinal manipulation. Given that each of these spinal manipulation modalities has been reported to produce therapeutic benefits, suggests that intersegmental motions produced by spinal manipulation may play an important role in eliciting therapeutic responses.

In a previous study Keller and Colloca [11] described a five segment, five DOF, lumped mass, lumbar spine model with a single displacement DOF (PA). These authors parametrically examined the effects of changes in the damping ratio (0.0–0.3) and PA stiffness (25–75 kN/m) of the FJS on the natural frequency of vibration and segmental and intersegmental displacement response under various loading conditions. They found that quasi-static and low frequency (<2.0 Hz) posterior–anterior forces (100 N) applied to the L3 vertebrae produced L3 segmental and L3–L4 inter-segmental PA displacements ranging from 2.7–8.1 mm and from 1.4–2.5 mm, respectively. Lumbar segment stiffness coefficients ranging from 25–60 kN/m and damping ratios from 0.15–0.25 were found to produce a combination of static, quasi-static (sinusoidal), and impulsive displacement responses that were most similar to in vivo experimental data reported in the literature. The current study expands upon this earlier work by including structures representing the thorax and pelvis, and by formulating the equations of motion to give three displacement DOF (PA, axial and FE rotation) with coupling between the axial and rotational axes. Compared to the aforementioned study, the results of the current model mirror the salient features of the previous findings. However, in the present study we found that the damped natural frequency of vibration for the PA axis was reduced by about 10% in comparison to the corresponding five DOF model. Segmental and intersegmental PA displacement magnitudes were also reduced by about 10%. Hence, the added mass, stiffness and damping parameters of the thorax and pelvis, together with additional DOF and coupling between axes acts to stiffen the spinal structure in the PA axis. Other parameters that will have an appreciable influence on the model results include K, M, ζ, l and a, but parametric examination of these parameters is beyond the scope of this study.

In this paper we have determined the posterior–anterior dynamic response of thorax, lumbar spine, and pelvis by considering these structures to be an assemblage of elements comprised of rigid structures (vertebral segments of uniform mass) connected by massless flexible linkages with three displacement DOF. Since the thorax-lumbar spine-pelvis was an assemblage of only seven structural elements, we were able to impose equilibrium considerations to assemble the system stiffness matrix in an analytical manner. Alternatively, one can use the finite element method, which involves the same procedures, but in a more systematic way. Namely, element coordinates and forces are first transformed into global coordinates and the stiffness matrix of the entire structure is then assembled into a global system of common orientation. Models based upon the finite element method are particularly useful for stress analysis, but can also be used for vibration analysis. However, from the standpoint of being able to duplicate the vibration mode shapes, the accuracy obtained from the finite element method is closely dependent on the number and type of elements used to define the structural joints. In general, many additional elements are required to obtain a good approximation of stresses or to obtain

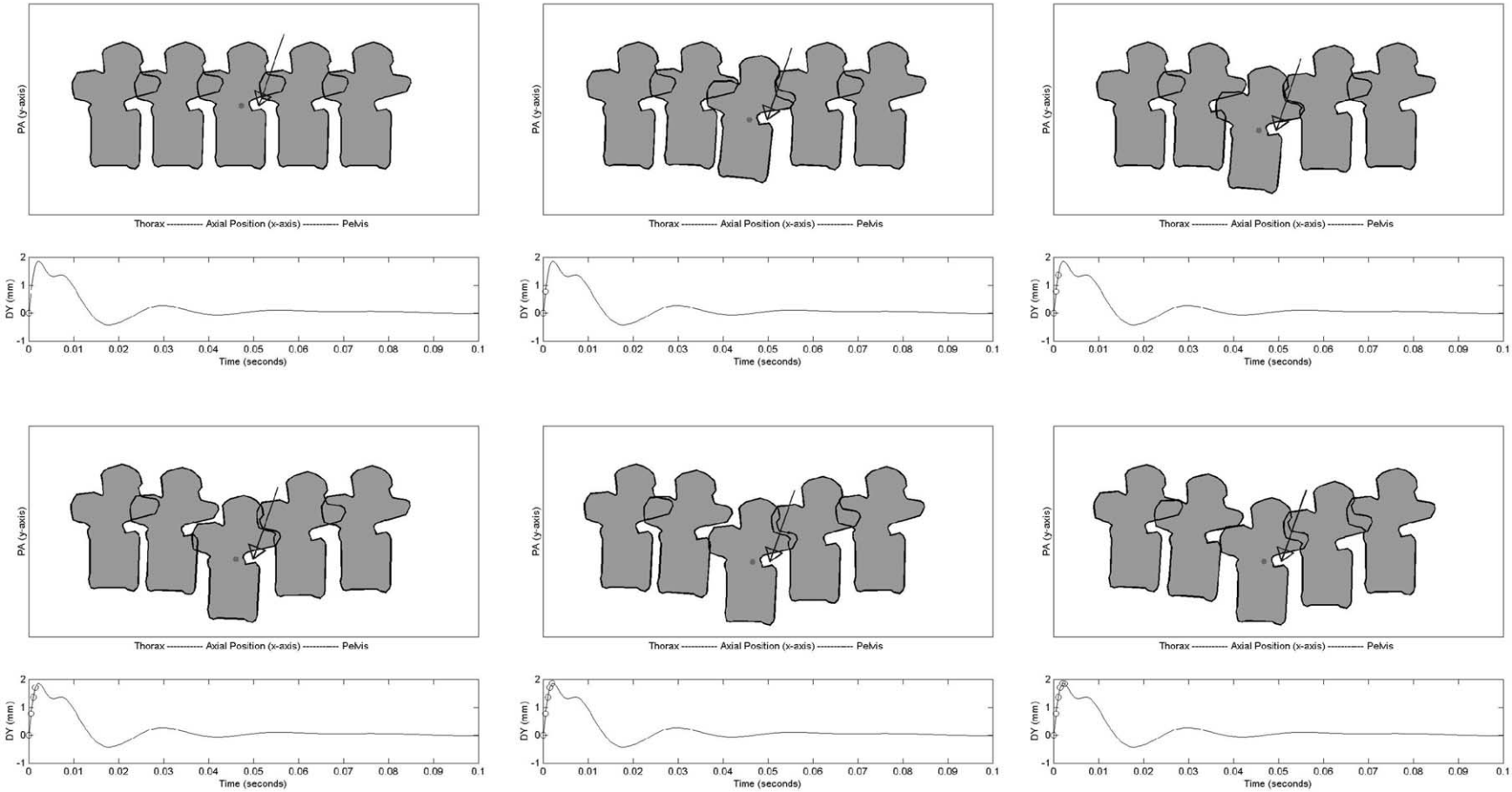

Fig. 6. Graphical simulation of the lumbar segmental motion response to an impulsive dynamic force at L3 $V_0 = 1.8414\ \mathrm{ms}^{-1}$, $\varphi = -20°$, $e = 0.01$ m. Panels (left to right, top to bottom) show 0.5 ms interval motion responses starting at time 0. Axial displacement, posterior–anterior displacement, and flexion–extension rotation have been magnified by factors of 10×, 10× and 5×, respectively. Line graph below each figure depicts the PA displacement–time history and corresponding time point (last open circle) for each figure.

accurate values for natural frequencies corresponding to the higher modes of vibration. Hence, an advantage of using a few structural elements defined according to stiffness influence coefficients over the finite element method lies in the increased accuracy and computer efficient nature of this approach.

There are inherent limitations of the current model. First, in specifying a single set of elastic coefficients for each vertebral segment, thorax and pelvis, and coordinate axis, we have greatly simplified the description of these FJS. In reality, the normal lumbar spine is comprised of a flexible anterior and posterior column, and has both passive structures (ligaments, cartilage) and active structures (skeletal muscle) that contribute to the biomechanical behavior. As currently formulated, therefore, we cannot examine the influence of the anterior and posterior columns separately on the mechanical response of the lumbar spine; nor can we examine the role that ligaments and muscle tone play in this regard, or when the spine is preloaded during manipulation. Rather, we are limited to examination of the general linear, static and dynamic mechanical responses of the spine. Moreover, the model does not take into account the complex geometry of the spine, including the lordotic curvature, which probably does not affect the vibration response appreciably, but may have a significant effect on the displacement response of the spine. In addition, in this model we have considered coupling of forces and moments between two axes when, in fact, forces and moments are coupled in all axes. Lastly, the model is currently limited to characterization of the mechanical response in the sagittal plane. Some spinal manipulative techniques apply forces in axial rotation and lateral translation in addition to PA translation with varying preload forces [15].

The model is general enough that it can easily be applied to the frontal plane simply by specifying appropriate stiffness and spring axis constants. Furthermore, the model can be generalized to account for six displacement DOF (three in the sagittal plane and three in the frontal plane). Although we have focused our analysis on the displacement response to forces applied to single segment, it is also important to note that the response to forces distributed over several segments can also be modeled. Moreover, the velocity and acceleration responses of the segments to sinusoidal and impulsive forces are easily obtained from the model. For purposes of clarity and brevity, however, we have limited our analysis to the displacement response resulting from static and dynamic forces delivered to a single segment.

Overall, the model predictions agree favorably with in vivo experimental data present in the literature. Noteworthy is the fact that the model reproduces the first resonant frequency (4–6 Hz) and gain (3–6 dB or 1.4–2.0×) observed in experimental studies of the seated and standing humans subjected to impact (impulsive) forces [26,27]. The model predicted PA axis undamped natural frequency (40.6 Hz) and damped natural frequency (39.3 Hz) of vibration also compare favorably with recent in vivo experimental data obtained for prone-lying human subjects using a driving-point mechanical impedance technique [28]. Keller et al. [28] found that PA impulsive forces delivered to the spinous processes of lumbar vertebrae produced PA oscillations with a natural frequency ranging from 38 to 41 Hz. In addition to studies of the vibration and impulsive force responses of the lumbar spine, a substantial number of in vivo PA mobilization studies have been performed in prone-lying human subjects using low frequency ($\leqslant$2.0 Hz), low force ($\leqslant$120 N) PA-directed oscillations applied to the spinous processes of lumbar vertebrae [16,18,20–22,24,29]. In these studies the main outcome measure is the PA stiffness of the lumbar vertebrae. Based on the range of L3 lumbar PA stiffness values reported in these studies (11.4–15.8 kN/m), PA vertebral segment displacements corresponding to a 100 N PA force range from 6.3 to 8.8 mm. Model-predicted static and quasi-static ($\leqslant$0.1 Hz) PA displacements obtained in this study (approximately 8 mm) agree with these experimental findings.

Posterior–anterior intersegmental motion responses are also of the same magnitude as inter-segmental motion responses produced during the application of in vivo posterior-anteriorly directed impulsive thrust, mechanical force, manually-assisted manipulative thrusts in three prone-lying human subjects [6]. Using a 3-DOF intervertebral motion device (IMD) attached directly to pins inserted into the spinous processes, Nathan and Keller [6] reported results for the peak-to-peak L3–L4 and L4–L5 intersegmental motion response to an approximately 90 N PA impulsive mechanical force, manually assisted thrust (<5 ms) delivered to various spinal segments (T12 to L3). In a group comprised of one normal and two surgical patients, intersegmental PA displacements, axial displacements and FE rotations ranged from 0.1 to 0.5 mm, 0.3 to 1.6 mm, and from 0.1 to 0.9°, respectively. In general, they found that the intersegmental displacements and rotations increased as the mechanical force, manually assisted forces were delivered closer to the IMD measurement site. In the present study, we have limited our analysis to the L3–L4 intersegmental motion response to forces delivered to the L3 vertebrae of an idealized or reference subject, so direct comparison to the IMD measurements of normal and pathologic subjects is not possible. However, our model predicted L3–L4 displacements and rotations associated with a 100 N peak PA impulsive force delivered at L3 agree well with the experimental findings of Nathan and Keller [6].

In a more recent study, Colloca et al. [25] reported the dynamic deformation response of four prone-lying

human subjects undergoing spinal decompressive surgery. PA and axial deformation were derived from acceleration–time recordings obtained from tri-axial accelerometers attached to pins inserted into the spinous processes of the patients. Dynamic mechanical force, manually assisted thrusts (~120 N, ~5 ms duration) delivered to spinous processes of vertebrae adjacent to the instrumented pins were found to elicit vertebral segment axial and transverse oscillations with peak–peak magnitudes ranging from 0.18 to 0.27 mm and from 0.29 to 0.52 mm, respectively. Differences between these experimental studies and the model predictions may reflect the age, gender and spinal degeneration of surgical patients examined in this series. Additional experimental data, quantifying segmental and intersegmental motions (displacement, velocity and acceleration) of normal and pathologic lumbar vertebrae in response to spinal manipulation and conditions that mimic spinal manipulation, are needed to better understand the biomechanical effects of lumbar spinal manipulation therapy and to further validate the model predictions.

When comparing previous experimental findings to the model results there are a number of additional factors that must be considered. First, the lumbar spine is a viscoelastic structure and therefore exhibits time-dependent behavior. As a result, quasi-static loading conditions will tend to overestimate the displacement response (underestimating the stiffness) due to creep deformation of the structure. Evidence of such behavior has been observed in studies reporting the PA motion response of the lumbar spine at different oscillation frequencies [20,22]. In these studies, quasi-static or slow cycling ($\leqslant$0.1 Hz) PA mobilization is associated with an approximately 15–25% increase in deformation (15–25% reduction in stiffness) in comparison to mobilization at 0.5–1.0 Hz. While the model presented in the current study contains viscous damping elements, the analysis does not consider flow-dependent or creep behavior of the spine.

Another important characteristic of the human lumbar spine is its nonlinear, load-deformation behavior. Inherent nonlinearities in the load-deformation characteristics of the spine result in variations in the measured PA displacement and stiffness that are dependent on the magnitude of the applied force. For example, previous PA mobilization studies have reported a substantial increase in PA stiffness when the peak force applied is increased [23,30]. In the current model, the nonlinear load-deformation behavior of the lumbar spine is not considered, and thus increases in the PA force will result in a proportional linear increase in deformation response. Thus, the motion response obtained for the 100 N forces examined in this study should not be extrapolated to higher forces typically associated with manual manipulation. However, one way to account for the nonlinear load-deformation behavior of the spine in the model would be to simply increase the segment stiffness. Moreover, as noted previously, we have not considered the role of muscle tension in the motion response of the lumbar spine. Lee and associates [31] found an approximately 3-fold increase in PA low cycle oscillatory stiffness for prone-lying subjects performing a maximum voluntary contraction in comparison to the resting state. The nonlinear, time-dependent and muscle stabilizing properties of the lumbar spine are very important when assessing the response of the spine to quasi-static and dynamic forces associated with manipulation therapy and assessment, and should be investigated further.

One of the interesting outcomes of this study was the finding that the PA segmental motion response of the lumbar vertebrae was relatively insensitive to both the thrust force angle and thrust force offset (contact point along the spinous process). We found that changes in the PA static, oscillatory and impulsive force displacement response became appreciable only at the highest thrust angle, and we also observed that the thrust force offset had only a minimal effect over the range of contact points examined. The former is consistent with findings obtained for low cycle PA mobilization of the prone-lying subject, wherein an increase in the thrust angle of $\pm 5°$ was found to produce less than a 2.5% change in force-deformation behavior, but an increase in the thrust angle of $\pm 10°$ changed the force-deformation response by up to 25% [16,22,24]. Our simulations suggest that axial displacements and FE rotations can change by 2-fold or more for thrust force angles greater than $-5°$ (caudal) in comparison to vertically oriented thrust forces (0°).

5. Conclusions

A structural model of the lumbar spine has been developed to characterize the sagittal plane static, sinusoidal and impulsive motion responses of lumbar spine segments. The model provides data on segmental and inter-segmental motion patterns that are otherwise difficult to obtain experimentally. Of potential clinical interest is the finding that the motion response of the spine is closely coupled to the frequency or the time history of the applied force. Namely, external mechanical forces applied at or near the natural frequency of the structure are associated with appreciably greater displacements (over 2-fold) in comparison to external forces that are static or quasi-static. Thus, it may be possible to achieve comparable posterior–anterior segmental motion responses for lower applied forces during spinal manipulation, provided that the forces are delivered over time intervals at or near the period corresponding to the natural frequency. Also of clinical interest is our observation that *intersegmental* motion responses asso-

ciated with quasi-static force–time histories (mobilization, manual manipulation) are quite similar to responses associated with dynamic force–time histories (mechanical force, manually assisted adjustments). Given the fact that highly disparate spinal manipulation modalities have been reported to produce therapeutic benefits [32], this observation suggests that intersegmental motions may play an important role in eliciting therapeutic responses.

Acknowledgements

Research supported, in part, by the National Institute of Chiropractic Research, Vermont Space Grant Consortium, NASA EPSCoR, Chiropractic Biophysics NonProfit, and the Foundation for the Advancement of Chiropractic Education.

Appendix A

Segment displacements are obtained from the solution to $\{F\} = [K]\{u\}$, where $\{F\}$ is force vector, $[K]$ is stiffness matrix, and $\{u\}$ is displacement vector:

$$K = \begin{bmatrix} K_{11} & K_{12} & K_{13} \\ K_{21} & K_{22} & K_{23} \\ K_{31} & K_{32} & K_{33} \end{bmatrix}, \quad F = \begin{Bmatrix} F_y \\ M_z \\ F_x \end{Bmatrix}, \quad u = \begin{Bmatrix} Y \\ \theta \\ X \end{Bmatrix},$$

where the system force vector is obtained from statics

$$\begin{aligned} F_{x_i} &= k_{x_i}[(X_i + \theta_i a_i) - (X_{i-1} + \theta_{i-1} a_{i-1})] \\ &\quad - k_{x_{i+1}}[(X_{i+1} + \theta_{i+1} a_{i+1}) - (X_i + \theta_i a_i)], \end{aligned}$$

$$\begin{aligned} F_{y_i} &= k_{y_i}\left[\left(Y_i - \frac{\theta_i l_i}{2}\right) - \left(Y_{i-1} + \frac{\theta_{i-1} l_{i-1}}{2}\right)\right] \\ &\quad - k_{y_{i+1}}\left[\left(Y_{i+1} - \frac{\theta_{i+1} l_{i+1}}{2}\right) - \left(Y_i + \frac{\theta_i l_i}{2}\right)\right], \end{aligned}$$

$$\begin{aligned} M_{z_i} &= \kappa_{z_i}(\theta_i - \theta_{i-1}) - \kappa_{z_i+1}(\theta_{i+1} - \theta_i) \\ &\quad + a_i k_{x_i}[(\chi_i + \theta_i a_i) - (\chi_{i-1} + \theta_{i-1} a_{i-1})] \\ &\quad - a_i k_{x_{i+1}}[(X_{i+1} + \theta_{i+1} a_{i+1}) - (X_i + \theta_i a_i)] \\ &\quad - \frac{l_i}{2} k_{y_i}\left[\left(Y_i - \frac{\theta_i l_i}{2}\right) - \left(Y_{i-1} + \frac{\theta_{i-1} l_{i-1}}{2}\right)\right] \\ &\quad - \frac{l_i}{2} k_{y_{i+1}}\left[\left(Y_{i+1} - \frac{\theta_{i+1} l_{i+1}}{2}\right) - \left(Y_i + \frac{\theta_i l_i}{2}\right)\right]. \end{aligned}$$

The system stiffness matrix is assembled using the following tri-diagonal matrix elements

$$\begin{aligned} K_{11} &= \left[-k_{y_i} \ (k_{y_i} + k_{y_{i+1}}) \ -k_{y_{i+1}}\right], \\ K_{12} &= \left[-k_{y_i}\frac{l_{i-1}}{2} \ \left(k_{y_{i+1}} - k_{y_i}\right)\frac{l_i}{2} \ k_{y_{i+1}}\frac{l_{i+1}}{2}\right], \\ K_{13} &= K_{31} = [0 \ 0 \ 0], \\ K_{21} &= \left[k_{y_i}\frac{l_i}{2} \ \left(k_{y_{i+1}} + k_{y_i}\right)\frac{l_i}{2} \ -k_{y_i+1}\frac{l_{i+1}}{2}\right], \\ K_{22} &= \left[\begin{Bmatrix} -\kappa_{z_i} \\ -a_i k_{x_i} a_{i-1} \\ +\frac{l_i k_{y_i} l_{i-1}}{4} \end{Bmatrix} \begin{Bmatrix} (\kappa_{z_i} + \kappa_{z_{i+1}}) \\ +a_i^2(k_{x_i} + k_{x_{i+1}}) \\ +\frac{(k_{y_{i+1}} + k_{y_i}) l_i^2}{4} \end{Bmatrix} \begin{Bmatrix} -\kappa_{z_{i+1}} \\ -a_i k_{x_{i+1}} a_{i+1} \\ +\frac{l_i k_{y_{i+1}} l_{i+1}}{4} \end{Bmatrix}\right], \\ K_{23} &= \left[-a_i k_{x_i} \ a_i(k_{x_i} + k_{x_{i+1}}) \ -a_i k_{x_{i+1}}\right], \\ K_{32} &= \left[-k_{x_i} a_{i-1} \ (k_{x_i} + k_{x_{i+1}}) a_i \ -k_{x_{i+1}} a_{i+1}\right], \\ K_{33} &= \left[-k_{x_i} \ (k_{x_i} + k_{x_{i+1}}) \ k_{x_{i+1}}\right], \end{aligned}$$

where $i =$ segment $1, \ldots, 7$, F is applied force, M is applied moment, k_x is axial stiffness, $k_y =$ PA stiffness, κ_z is torsion (FE rotation) stiffness, a is spring axis (x–z) constant, l is segment link dimension, θ is FE rotation angle, X is x-axis displacement, and Y is y-axis displacement. Each element of K_{22} has three components.

References

[1] Herzog W. Clinical biomechanics of spinal manipulation. Philadelphia: Churchill Livingstone; 2000.
[2] Lee R, Evans J. An in vivo study of the intervertebral movements produced by posteroanterior mobilization. Clin Biomech 1997;12:400–8.
[3] Herzog W, Conway PJ, Kawchuk GN, Zhang Y, Hasler EM. Forces exerted during spinal manipulative therapy. Spine 1993;18:1206–12.
[4] Triano J. The mechanics of spinal manipulation. In: Herzog W, editor. Clinical biomechanics of spinal manipulation. Philadelphia: Churchill Livingstone; 2000. p. 92–190.
[5] Keller TS, Colloca CJ, Fuhr AW. Validation of the force and frequency characteristics of the activator adjusting instrument: effectiveness as a mechanical impedance measurement tool. J Manipulative Physiol Ther 1999;22:75–86.
[6] Nathan M, Keller TS. Measurement and analysis of the in vivo posteroanterior impulse response of the human thoracolumbar spine: a feasibility study. J Manipulative Physiol Ther 1994;17:431–41.
[7] Keller TS, Colloca CJ, Fuhr AW. In vivo transient vibration assessment of the normal human thoracolumbar spine. J Manipulative Physiol Ther 2000;23:521–30.
[8] Lee M, Kelly DW, Steven GP. A model of spine, ribcage and pelvic responses to a specific lumbar manipulative force in relaxed subjects. J Biomech 1995;28:1403–8.
[9] Lee M, Lau H, Lau T. Sagittal plane rotation of the pelvis during lumbar posteroanterior loading. J Manipulative Physiol Ther 1994;17:149–55.
[10] Solinger AB. Theory of small vertebral motions: an analytical model compared to data. Clin Biomech 2000;15:87–94.
[11] Keller TS, Colloca CJ. A rigid body model of the dynamic posteroanterior motion response of the human lumbar spine. J Manipulative Physiol Ther 2002 [in press].
[12] Panjabi MM, White III AA. Physical properties and functional biomechanics of the spine. In: White A, Panjabi MM, editors. Clinical biomechanics of the spine. second ed. Philadelphia: Lippincott–Raven; 1990. p. 3–83.

[13] Keller TS, Nathan M. Height change caused by creep in intervertebral discs: a sagittal plane model. J Spinal Disord 1999;12:313–24.
[14] Schultz AB. Spine biomechanics. In: Mow VC, Hayes WC, editors. Basic orthopaedic biomechanics. Philadelphia: Lippincott–Raven; 1997. p. 383–4.
[15] Haldeman S, Chapman-Smith D, Petersen DM. Guidelines for chiropractic quality assurance and practice parameters. Gaithersburg, MD: Aspen Publishers; 1993.
[16] Caling B, Lee M. Effect of direction of applied mobilization force on the posteroanterior response in the lumbar spine. J Manipulative Physiol Ther 2001;24:71–8.
[17] Lee M, Svensson NL. Measurement of stiffness during simulated spinal physiotherapy. Clin Phys Physiol Meas 1990;11:201–7.
[18] Allison GT, Edmondston SJ, Roe CP, Reid SE, Toy DA, Lundgren HE. Influence of load orientation on the posteroanterior stiffness of the lumbar spine. J Manipulative Physiol Ther 1998;21:534–8.
[19] Gal J, Herzog W, Kawchuk G, Conway PJ, Zhang YT. Movements of vertebrae during manipulative thrusts to unembalmed human cadavers. J Manipulative Physiol Ther 1997;20:30–40.
[20] Lee M, Svensson NL. Effect of loading frequency on response of the spine to lumbar posteroanterior forces. J Manipulative Physiol Ther 1993;16:439–46.
[21] Lee M, Latimer J, Maher C. Manipulation: investigation of a proposed mechanism. Clin Biomech 1993;8:302–6.
[22] Lee M, Liversidge K. Posteroanterior stiffness at three locations in the lumbar spine. J Manipulative Physiol Ther 1994;17:511–6.
[23] Lee M, Latimer J, Maher C. Normal response to large posteroanterior lumbar loads – a case study approach. J Manipulative Physiol Ther 1997;20:369–71.
[24] Viner A, Lee M, Adams R. Posteroanterior stiffness in the lumbosacral spine. The correlation between adjacent vertebral levels. Spine 1997;22:2724–9.
[25] Colloca CJ, Keller TS, Gunzburg R. Toward an understanding of the chiropractic adjustment: a neuromechanical model derived from original data. In: Proceedings of the Sixth Biennial Congress of the World Federation of Chiropractic. Toronto, Ontario: The World Federation of Chiropractic; 2001. p. 261–3.
[26] Broman H, Pope MH, Benda M, Svensson M, Ottosson C, Hansson T. The impact response of the seated subject. J Orthop Res 1991;9:150–4.
[27] Pope MH, Magnusson M, Hansson T. The upper extremity attenuates intermediate frequency vibrations. J Biomech 1997;30:103–8.
[28] Keller TS, Colloca CJ, Fuhr AW. In vivo transient vibration analysis of the normal human thoracolumbar spine. J Manipulative Physiol Ther 2000;23:521–30.
[29] Latimer J, Goodsel MM, Lee M, Maher CG, Wilkinson BN, Moran CC. Evaluation of a new device for measuring responses to posteroanterior forces in a patient population, Part 1: Reliability testing. Phys Ther 1996;76:158–65.
[30] Latimer J, Lee M, Adams RD. The effects of high and low loading forces on measured values of lumbar stiffness. J Manipulative Physiol Ther 1998;21:157–63.
[31] Lee M, Esler M-A, Mildren J. Effect of extensor muscle activation on the response to lumbar posteroanterior forces. Clin Biomech 1993;8:115–9.
[32] Koes BW, Assendelft WJ, van der Heijden GJ, Bouter LM. Spinal manipulation for low back pain. An updated systematic review of randomized clinical trials. Spine 1996;21:2860–71.